CACNA1H Mutations Are Associated With Different Forms of Primary Aldosteronism

Georgios Daniil, Fabio L. Fernandes-Rosa, Jean Chemin, Iulia Blesneac, Jacques Beltrand, Michel Polak, Xavier Jeunemaitre, Sheerazed Boulkroun, Laurence Amar, T. M. Strom, et al.

EBioMedicine 13 (2016) 225–236

Contents lists available at ScienceDirect

EBioMedicine

journal homepage: www.ebiomedicine.com

Research Paper

CACNA1H Mutations Are Associated With Different Forms of Primary Aldosteronism

Georgios Daniil [a,b,1], Fabio L Fernandes-Rosa [a,b,c,*,1], Jean Chemin [d,e], Iulia Blesneac [d,e], Jacques Beltrand [b,f,g,h], Michel Polak [b,f,g,h], Xavier Jeunemaitre [a,b,c], Sheerazed Boulkroun [a,b], Laurence Amar [a,b,i], Tim M Strom [j,k], Philippe Lory [d,e], Maria-Christina Zennaro [a,b,c,*]

[a] INSERM, UMRS_970, Paris Cardiovascular Research Center, Paris, France
[b] Université Paris Descartes, Sorbonne Paris Cité, Paris, France
[c] Assistance Publique-Hôpitaux de Paris, Hôpital Européen Georges Pompidou, Service de Génétique, Paris, France
[d] Institut de Génomique Fonctionnelle, Université de Montpellier, CNRS UMR 5203, INSERM U 1191, Montpellier F-34094, France
[e] LabEx Ion Channel Science and Therapeutics, Montpellier F-34094, France
[f] Assistance Publique-Hôpitaux de Paris, Hôpital Necker Enfants Malades, Service d'Endocrinologie, Paris, France
[g] Inserm UMR_1016, Institut Cochin, Paris, France
[h] Institut Imagine, Paris Descartes – Université Sorbonne Paris Cité, Paris, France
[i] Assistance Publique-Hôpitaux de Paris, Hôpital Européen Georges Pompidou, Unité Hypertension artérielle, Paris, France
[j] Institute of Human Genetics, Helmholtz Zentrum München, Neuherberg, Germany
[k] Institute of Human Genetics, Technische Universität München, Munich, Germany

ARTICLE INFO

Article history:
Received 18 August 2016
Received in revised form 22 September 2016
Accepted 3 October 2016
Available online 4 October 2016

Keywords:
Adrenal
Aldosterone producing adenoma
Familial hyperaldosteronism
Early onset hyperaldosteronism
Voltage dependent calcium channel
Hypertension

ABSTRACT

Primary aldosteronism (PA) is the most common form of secondary hypertension. Mutations in *KCNJ5*, *ATP1A1*, *ATP2B3* and *CACNA1D* are found in aldosterone producing adenoma (APA) and familial hyperaldosteronism (FH). A recurrent mutation in *CACNA1H* (coding for Cav3.2) was identified in a familial form of early onset PA. Here we performed whole exome sequencing (WES) in patients with different types of PA to identify new susceptibility genes.

Four different heterozygous germline *CACNA1H* variants were identified. A de novo Cav3.2 p.Met1549Ile variant was found in early onset PA and multiplex developmental disorder. Cav3.2 p.Ser196Leu and p.Pro2083Leu were found in two patients with FH, and p.Val1951Glu was identified in one patient with APA. Electrophysiological analysis of mutant Cav3.2 channels revealed significant changes in the Ca^{2+} current properties for all mutants, suggesting a gain of function phenotype. Transfections of mutant Cav3.2 in H295R-S2 cells led to increased aldosterone production and/or expression of genes coding for steroidogenic enzymes after K^+ stimulation. Identification of *CACNA1H* mutations associated with early onset PA, FH, and APA suggests that *CACNA1H* might be a susceptibility gene predisposing to PA with different phenotypic presentations, opening new perspectives for genetic diagnosis and management of patients with PA.

1. Introduction

Primary aldosteronism (PA) is the most common form of secondary arterial hypertension, with an estimated prevalence of ~10% in referred patients, 4% in primary care (Hannemann and Wallaschofski, 2012), and 20% in patients with resistant hypertension (Calhoun et al., 2002; Douma et al., 2008). It is characterised by hypertension, hypokalemia, and inadequate high levels of plasma aldosterone for low levels of plasma renin (Funder et al., 2016). Aldosterone-producing adenoma (APA) or bilateral adrenal hyperplasia (BAH) are the most frequent causes of PA (Amar et al., 2010).

Somatic mutations in *KCNJ5* (encoding the potassium channel GIRK4), *ATP1A1* (encoding the α1 subunit of the Na^+/K^+-ATPase), *ATP2B3* (encoding the plasma membrane Ca^{2+}-ATPase, type 3 PMCA3), and *CACNA1D* (encoding the α1 subunit of the L-type voltage-dependent calcium channel Cav1.3) were identified in ≈50% of APA (Azizan et al., 2013; Beuschlein et al., 2013; Choi et al., 2011; Fernandes-Rosa et al., 2014; Scholl et al., 2013). *KCNJ5* and *ATP1A1* mutations are responsible for chronic zona glomerulosa cell membrane depolarization leading to opening of voltage-dependent calcium channels, while *ATP2B3* mutations affect intracellular calcium recycling and *CACNA1D* mutations lead

Abbreviations: PA, primary aldosteronism; APA, aldosterone producing adenoma; FH, familial hyperaldosteronism; WES, whole exome sequencing.

* Corresponding authors at: INSERM, U970, Paris Cardiovascular Research Center – PARCC, 56, rue Leblanc, 75015 Paris, France.
E-mail addresses: fabio.fernandes-rosa@inserm.fr (F.L. Fernandes-Rosa), maria-christina.zennaro@inserm.fr (M.-C. Zennaro).

[1] Equal contribution.

http://dx.doi.org/10.1016/j.ebiom.2016.10.002

to voltage-dependent calcium channel activation and opening at lower voltages (Azizan et al., 2013; Beuschlein et al., 2013; Choi et al., 2011; Scholl et al., 2013). All these genetic abnormalities converge towards increasing intracellular calcium concentration with activation of calcium signaling triggering increased expression of *CYP11B2* encoding aldosterone synthase, which catalyzes the last steps of aldosterone biosynthesis.

While the majority of cases of PA are sporadic, 1–5% of cases are familial forms (Zennaro et al., 2015). Familial hyperaldosteronism (FH) type I is a disease with autosomal dominant transmission due to unequal crossing-over of genetic material between the genes coding for aldosterone synthase (*CYP11B2*) and 11β-hydroxylase (*CYP11B1*). Thus aldosterone biosynthesis is regulated by ACTH resulting in a circadian pattern of aldosterone production which parallels that of cortisol production and which is suppressible by dexamethasone (Sutherland et al., 1966). FH type II (FH-II) is not remediable by glucocorticoids and is diagnosed on the basis of two or more affected family members in the absence of the chimeric *CYP11B1/CYP11B2* gene. The genetic cause of FH-II is still unknown, but a linkage to chromosomal region 7p22 has been established in some families (Lafferty et al., 2000; So et al., 2005; Sukor et al., 2008). Recurrent germline mutations in *KCNJ5* (Adachi et al., 2014; Charmandari et al., 2012; Choi et al., 2011; Monticone et al., 2013; Mulatero et al., 2012; Scholl et al., 2012) were identified in FH type III (FH-III) and are associated with phenotypes of different severity. De novo germline *CACNA1D* mutations were described in two children with PASNA (Primary aldosteronism, seizures, and neurological abnormalities), a syndrome featuring PA and neuromuscular abnormalities (Scholl et al., 2013). More recently, a recurrent germline mutation in *CACNA1H* (encoding the pore-forming α1 subunit of the T-type voltage-dependent calcium channel Cav3.2) (p.Met1549Val) was identified in 5 children with PA before age 10. Familial analysis revealed autosomal dominant transmission of *CACNA1H* mutations with incomplete penetrance and a new form of familial PA (Scholl et al., 2015).

Despite these recent advances, the pathogenesis of a large proportion of sporadic and familial cases of PA has not been elucidated. The aim of the present study was to identify new genetic abnormalities in patients with PA. To this purpose we have performed whole exome sequencing (WES) in patients with different types of PA. We identified four germline variations in *CACNA1H* which affect the electrophysiological and functional properties of the channel, leading to increased *CYP11B2* expression and aldosterone production.

2. Subjects and Methods

2.1. Patients

Patients with PA were recruited between 1994 and 2012 within the COMETE (COrtico-et MEdullo-surrénale, les Tumeurs Endocrines) network or in the context of genetic screening for familial hyperaldosteronism at the genetics department of the HEGP. Methods for screening and subtype identification of PA were performed according to institutional and Endocrine Society guidelines (Funder et al., 2008; Letavernier et al., 2008). In patients diagnosed with primary aldosteronism, a thin slice CT scan or MRI of the adrenal and/or an adrenal venous sampling (AVS) were performed to differentiate between unilateral and bilateral aldosterone hypersecretion. All patients gave written informed consent for genetic and clinical investigation. Procedures were in accordance with institutional guidelines. The diagnosis of adrenocortical adenoma was histologically confirmed after surgical resection. A final diagnosis of APA, diagnosed by CT scanning and AVS, was considered "proven" when the following conditions were satisfied: 1) histological demonstration of adenoma; 2) normalization of hypokalemia, if present; 3) cure or improvement of hypertension; 4) normalization of ARR and/or suppressibility of aldosterone under saline load (Mulatero et al., 2009; Rossi et al., 2006). All patients gave written informed consent for genetic and clinical investigation within each individual institution. Procedures were in accordance with institutional guidelines.

2.2. DNA Isolation

Tumor DNA was extracted using QIAamp DNA midi kit (Qiagen, Courtaboeuf Cedex, France). DNA from peripheral blood leukocytes was prepared using salt-extraction.

2.3. Whole Exome Sequencing and Variant Detection

Exomes were enriched in solution and indexed with SureSelect XT Human All Exon 50 Mb kits (Agilent). Sequencing was performed as 100 bp paired-end runs on HiSeq2000 systems (Illumina). Pools of 12 indexed libraries were sequenced on four lanes. Image analysis and base calling was performed using Illumina Real Time Analysis. CASAVA 1·8 was used for demultiplexing. BWA (v 0.5.9) with standard parameters was used for read alignment against the human genome assembly hg19 (GRCh37). We performed single-nucleotide variant and small insertion and deletion (indel) calling specifically for the regions targeted by the exome enrichment kit, using SAMtools (v 0.1.18). Subsequently the variant quality was determined using the SAMtools varFilter script. We used default parameters, with the exception of the maximum read depth (-D) and the minimum *P*-value for base quality bias (−2), which we set to 9999 and 1e-400, respectively. Additionally, we applied a custom script to mark all variants with adjacent bases of low median base quality. All variants were then annotated using custom Perl scripts. Annotation included information about known transcripts (UCSC Known Genes and RefSeq genes), known variants (dbSNP v 135), type of mutation, and - if applicable – amino acid change in the corresponding protein. The annotated variants were then inserted into our in-house database.

To discover putative somatic variants, we queried our database to show only those variants of a tumor that were not found in the corresponding control tissue. To reduce false positives we filtered out variants that were already present in our database, had variant quality <40, or failed one of the filters from the filter scripts. We then manually investigated the raw read data of the remaining variants using the Integrative Genomics Viewer (IGV).

2.4. Sanger Sequencing

CACNA1H DNA was amplified using intron-spanning primers described in Supplemental Table S1. PCR was performed on 100 ng of DNA in a final volume of 25 μL containing 0.75 mM $MgCl_2$, 400 nM of each primer, 200 μM deoxynucleotide triphosphate, and 1.25 U Taq DNA Polymerase (Sigma). Cycling conditions for *CACNA1H* were as previously described (Hubert et al., 2011) with an annealing temperature of 60 °C. Direct sequencing of PCR products was performed using the ABI Prism Big Dye Terminator® v3.1 Cycle Sequencing Kit (Applied Biosystems, Foster City, CA) on an ABI Prism 3700 DNA Analyzer (Applied Biosystems).

2.5. Site Directed Mutagenesis

The $Cav3.2_{196Leu}$, $Cav3.2_{1549Ile}$, $Cav3.2_{1951Glu}$ and $Cav3.2_{2083Leu}$ constructs, coding for the mutant forms of Cav3.2 were generated by site-directed mutagenesis using the QuikChange II XL site-directed mutagenesis kit (Agilent). The mutations were introduced into the human Cav3.2 HA cDNA fragment inserted into pcDNA3.1 (Dubel et al., 2004) and their presence confirmed by Sanger sequencing.

2.6. Cell Culture and Transfection Protocols

tsA-201 cells were cultivated in DMEM supplemented with GlutaMax, 10% fetal bovine serum and 1% penicillin/streptomycin (Invitrogen). Transfections were performed using jet-PEI (QBiogen) with a DNA mix (1.5 μg total) containing 0.5% of a GFP encoding plasmid and 99.5% of either of the plasmid constructs coding either for the wild-

type or the mutant human Cav3.2 T-type channels. Two days after transfection, tsA-201 cells were dissociated with Versene (Invitrogen) and plated at a density of ~35×10^3 cells per 35 mm Petri dish for electrophysiological recordings, which were performed the following day.

The human adrenocortical carcinoma cell line H295R strain 2 (H295R-S2) was kindly provided by W. E. Rainey (Wang et al., 2012). H295R-S2 cells were cultured in DMEM/Eagle's F12 medium (GIBCO, Life technologies, Carlsbad, CA) supplemented with 2% Ultroser G (PALL life sciences, France), 1% insulin/transferrin/selenium Premix (GIBCO, Life technologies, Carlsbad, CA), 10 mM HEPES (GIBCO, Life technologies, Carlsbad, CA), 1% penicillin, and streptomycin (GIBCO, Life technologies, Carlsbad, CA) and maintained in a 37 °C humidified atmosphere (5% CO2).

2.7. Electrophysiological Recordings

Macroscopic currents were recorded at room temperature using an Axopatch 200B amplifier (Molecular Devices). Borosilicate glass pipettes had a resistance of 1.5–2.5 M Ohm when filled with an internal solution containing (in mM): 140 CsCl, 10 EGTA, 10 HEPES, 3 Mg-ATP, 0.6 GTPNa, and 3 $CaCl_2$ (pH adjusted to 7.25 with KOH, ~315 mOsm, ~100 nM free Ca^{2+} using the MaxChelator software, http://maxchelator.stanford.edu/). The extracellular solution contained (in mM): 135 NaCl, 20 TEACl, 2 $CaCl_2$, 1 $MgCl_2$, and 10 HEPES (pH adjusted to 7.25 with KOH, ~330 mOsm). Recordings were filtered at 5 kHz. Current–voltage curves (I–V curves) were fitted using a combined Boltzmann and linear Ohmic relationships, where $I = Gmax \times (Vm - Vrev) / (1 + \exp((Vm - V0.5) / \text{slope factor}))$. Similarly, steady-state inactivation curves were fitted using the Boltzmann equation where $I/I\,max = 1/(1 + \exp((Vm - V0.5) / \text{slope factor}))$. Data were analyzed using pCLAMP9 (Molecular Devices, Sunnyvale, CA) and GraphPad Prism (GraphPad software Inc., San Diego, CA) software. Results were presented as the mean ± SEM, and n was the number of cells.

2.8. Functional Studies in H295R-S2

For functional experiments, H295R-S2 cells were seeded to tissue culture dishes 100 in groups of 4,000,000 cells per dish, and maintained at the conditions described. After 24 h, cells were transfected with WT or mutant forms of *CACNA1H* ($Cav3.2_{196Leu}$, $Cav3.2_{1549Ile}$, $Cav3.2_{1951Glu}$, and $Cav3.2_{2083Leu}$) using Effectene (Qiagen, Valencia, CA). 24 h post transfection, cells were transferred in 24 well-plates and serum deprived in DMEM/F12 containing 0.1% Ultroser G for 24 h and then incubated for another 24 h with fresh medium containing 0.1% Ultroser G with no secretagogue (basal) or 10 nM of AngII (A-II 10 nM), or 12 mM K^+ (K^+ 12 mM). At the end of this incubation time, supernatant and cells from each well were harvested for aldosterone measurement and RNA extraction. For each mutant, three experiments were independently conducted in triplicates or quadriplicates.

2.9. RNA Extraction and RT-qPCR

Total RNA was extracted in Trizol reagent (Ambion Life technologies, Carlsbad CA) according to the manufacturer's recommendations. After deoxyribonuclease I treatment (Life Technologies, Carlsbad, CA), 500 ng of total RNA was retrotranscribed (iScript reverse transcriptase, Biorad, Hercules, CA). Primers used for qPCR are described in Table S2. The quantitative PCR was performed using SYBRgreen (Sso advanced universal SyBr Green supermix, Biorad, Hercules, CA) on a C1000 touch thermal cycler of Biorad (CFX96 Real Time System), according to the manufacturer's instructions. Controls without template were included to verify that fluorescence was not overestimated from primer dimer formation or PCR contaminations. RT-qPCR products were analyzed in a post amplification fusion curve to ensure that a single amplicon was obtained. Normalization for RNA quantity, and reverse transcriptase efficiency was performed against three reference genes (geometric mean of the expression of Ribosomal 18S RNA, HPRT, and GAPDH), in accordance with the MIQE guidelines (Bustin et al., 2009). *CACNA1H* expression was quantified to normalize for transfection efficiency. Quantification was performed using the standard curve method. Standard curves were generated using serial dilutions from a cDNA pool of all samples of each experiment, yielding a correlation coefficient of at least 0.98 in all experiments.

2.10. Aldosterone and Protein Assays

Aldosterone levels were measured in cell culture supernatants by ELISA. Aldosterone antibody and aldosterone-3-CMO-biotin were kindly provided by Dr Gomez-Sanchez (Gomez-Sanchez et al., 1987). Aldosterone concentrations were normalized to cell protein concentration (determined using Bradford protein assay) and *CACNA1H* expression.

2.11. Statistical Analyses

Quantitative variables are reported as means ± standard deviation when Gaussian distribution or medians and interquartile range when no Gaussian distribution, and compared with unpaired *t*-test or Mann-Whitney test respectively. Multiple comparisons were analyzed by one-way ANOVA followed by Bonferroni test. Statistical analysis of electrophysiological measures were performed with one-way ANOVA combined with a Tukey post-test ($^*P < 0.05$, $^{**}P < 0.01$, $^{***}P < 0.001$). Categorical variables are reported as percentages and compared with Fisher's exact test. A P value < 0.05 was considered significant for comparisons between 2 groups. For functional experiments, all results were expressed as mean ± SEM of at least three separate experiments performed in triplicate or quadruplicate. Analyses were performed using Prism5 (GraphPad software Inc., San Diego, CA).

3. Results

3.1. Whole Exome Sequencing in Patients With PA

In order to identify new genes in PA, WES was performed on germline DNA from a young patient with early onset hypertension and hyperaldosteronism and his parents under the hypothesis of a de novo mutation. Whole exome sequencing was also performed in 10 subjects from the French West Indies with a family history of hypertension and PA under the hypothesis of a founder effect. For all these patients the presence of the chimeric *CYP11B1/CYP11B2* gene and of recurrent *KCNJ5* mutations had been excluded. We sought previously unreported (dbSNP, Helmholtz exome database) and protein altering variants in genes that occurred in more than one subject. Among germline variants observed with this approach, we identified three missense variants in the *CACNA1H* gene, coding for the pore-forming subunit of Cav3.2, affecting conserved residues of the protein (Fig. 1A–C). All variants were confirmed by Sanger sequencing of independent DNA samples (Fig. 1A–C).

The germline *CACNA1H* variant c.4647G>C (p.Met1549Ile) was identified in subject K055-3 but not in his asymptomatic parents (K055-1 and K055-2), suggesting a de novo mutation responsible for his phenotype (Fig. 1A). This variant was absent among >120,000 alleles sequenced from diverse populations in the Exome Aggregation Consortium (ExAC) and the Helmholtz exome databases. The variation *CACNA1H* p.Met1549Ile is located in the transmembrane segment S6 of the repeat domain III of Cav3.2 (Fig. 1A and E) and modifies the same amino acid as the *CACNA1H* p.Met1549Val variant recently reported in FH-IV (Scholl et al., 2015).

The germline *CACNA1H* variation c.587C>T (p.Ser196Leu) was identified in subject K475-1 with a family history of PA (Table 1). The same variant was identified by Sanger sequencing in one sister (K475-2) who also presented resistant hypertension and PA (Fig. 1B). The variant affects an amino acid located in the voltage sensor region on the

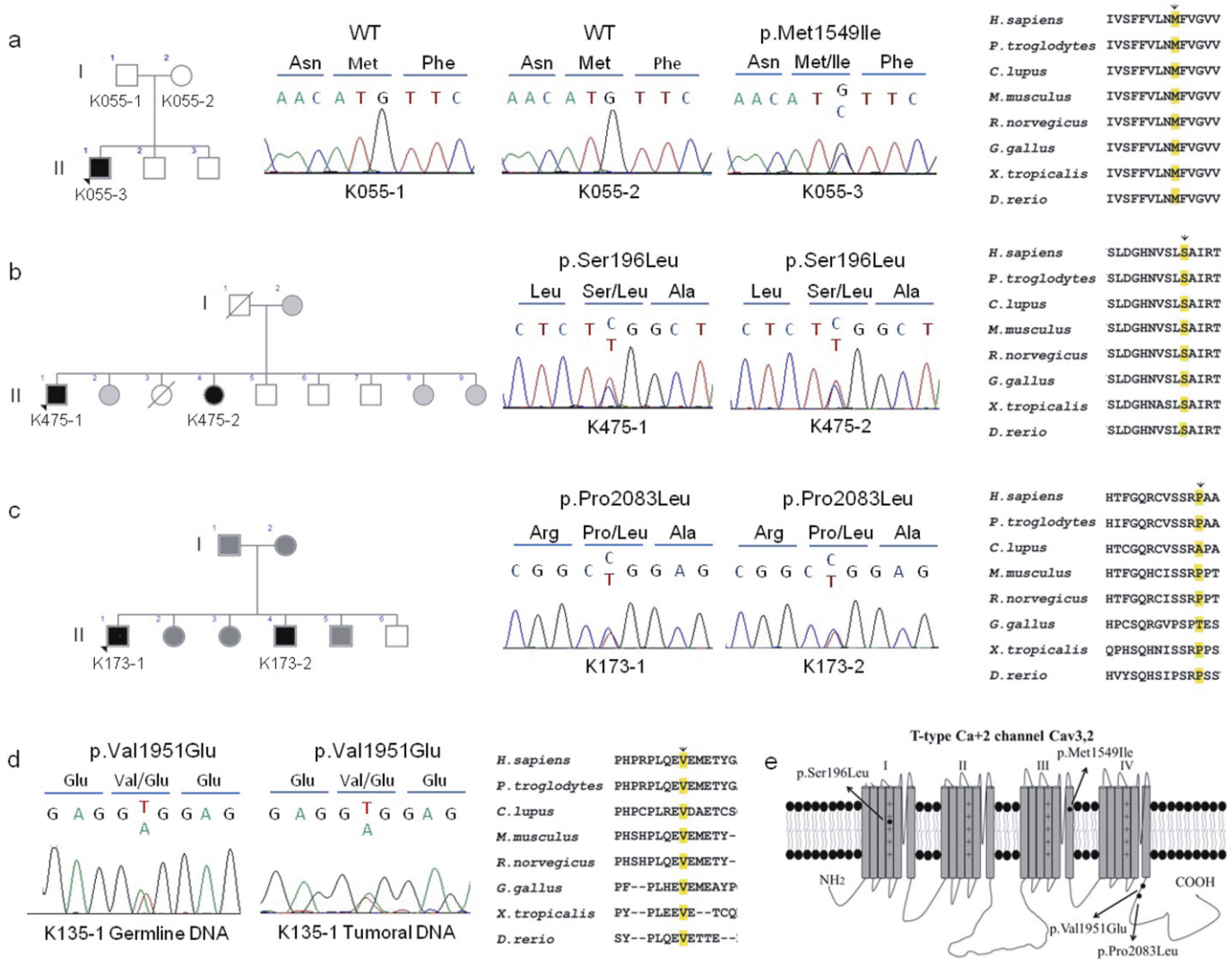

Fig. 1. *CACNA1H* variations identified in patients with PA. A–D. Pedigrees, Sanger sequencing chromatograms, alignment, and conservation of residues encoded by *CACNA1H* orthologs. A. c.4647G>C (p.Met1549Ile); B. c.587C>T (p.Ser196Leu); C. c.6248C>T (p.Pro2083Leu); D. c.5852T>A (p.Val1951Glu). Subjects with PA are shown with black symbols, subjects with arterial hypertension with grey symbols and non-affected subjects are shown with white symbols. E. Transmembrane structure of Cav3.2 representing the four homologous domains I–IV each with six transmembrane spans (Segments (S) 1–6), and cytoplasmic N- and C-termini. The pore of T-type channels is formed by the tetrameric arrangement of the four domains and is lined by the S6 segment in the intracellular part, while the S4 segment serves as the voltage sensor. The Met1549Ile mutation is located in S6 of repeat III and p.Ser196Leu in S4 of repeat I; p.Pro2083Leu and p.Val1951Glu are located in the C-terminal cytoplasmic domain.

transmembrane segment S4 of the repeat domain I of Cav3.2 (Fig. 1E). This variant was absent from the ExAC and Helmholtz exome databases. A third *CACNA1H* variant c.6248C>T, changing Proline 2083 into Leucine, was identified in a second subject with a family history of PA (K173-1, Fig. 1C); this variant is extremely rare, as it was found in 3 out of 92090 alleles in ExAC. Pro2083Leu is located in the C-terminal cytoplasmic domain of Cav3.2 (Fig. 1E) and was also identified in one brother (K173-2) diagnosed with PA (Fig. 1C).

To investigate whether *CACNA1H* could also be involved in PA associated with APA, we retrieved WES data from 23 patients with APA without known recurrent somatic mutations. A germline *CACNA1H* missense variant (c.5852T>A/p.Val1951Glu) was found in one patient with APA (subject K135-1). This variation was confirmed by Sanger sequencing both in germline and somatic APA DNA (Fig. 1D); its frequency is 3/18506 alleles in ExAC, whereas it is absent from the Helmholtz database. It is located in the C-terminal cytoplasmic domain of Cav3.2, in a region possibly implicated in fast channel activation. Similar to the other variants it affects a highly conserved residue of Cav3.2 (Fig. 1D and E).

Table 1
CACNA1H variations identified in patients with PA.

Patient	Form of PA	Variant cDNA	Variant protein	Domain
K055-3	Young onset	c.4647G>C	p.Met1549Ile	Tm S6, repeat III
K475-1	FH-II	c.587C>T	p.Ser196Leu	Tm S4, repeat I
K173-1	FH-II	c.6248C>T	p.Pro2083Leu	Cytoplasmic
K135-1	Sporadic APA	c.5852T>A	p.Val1951Glu	Cytoplasmic

TM: transmembrane; FH-II: familial hyperaldosteronism type II; NM_02198; NP_066921.

3.2. Clinical Features of Patients With CACNA1H Variants

Clinical and biochemical characteristics of subjects carrying *CACNA1H* variants are described in Table 2.

Subject K055-3 is a 22 year old male of European ancestry. At age 2 months, he underwent a pyloromyotomy to treat a pyloric stenosis. In the days following the discharge, the child was readmitted because of ENT infection and a major hypokalemia (1,7 mmol/L) associated to metabolic acidosis was discovered. Evaluation revealed high plasma aldosterone (3324 pmol/L; NV for age: 140-2500 pmol/L) despite suppressed renin (<1 mUI/L), and arterial hypertension. The diagnosis

Table 2
Patients characteristics.

	K055-3	K475-1	K475-2	K173-1	K173-2	K135-1
Sex	M	M	F	M	M	F
Form of PA	Early-onset	FH-II	FH-II	FH-II	FH-II	Sporadic, APA
Age at HTN dg	2 m	36 y	32 y	34 y	37 y	48 y
Age at PA dg	2 m	51 y	37 y	44 y	39 y	50 y
SBP at PA dg (mmHg)	110	155	153	154	160	142
DBP at PA dg (mmHg)	70	95	97	104	98	87
BMI at PA dg (kg/m^2)	–	27.8	32.4	25.8	34.7	23.4
Lowest plasma K^+ (mmol/l)	1.7	2.7	2.9	3.9	2.9	2.5
Urinary aldosterone[a] (nmol/24 h)	–	104	–	–	–	118
Plasma aldosterone (pmol/l)[b]	3324	965	804	753	688	620
Plasma renin (mU/l)	<1	3.7	2.6	3	<1	1.5
ARR (pmol/mU)[c]	624	193	160.8	150.6	137.6	124
Adrenal abnormalities on CT	No	Bilateral nodules	no	No	Left adrenal hyperplasia	Left adrenal nodule
AVS lateralisation index	–	48 (left)	–	–	–	–
Adenoma size (mm)	–	11	–	–	–	8

PA: primary aldosteronism; dg: diagnosis; m, months; y, years; HTN: hypertension; SBP: systolic blood pressure; DBP: diastolic blood pressure; BMI: body mass index; K: potassium; ARR: aldosterone to renin ratio; AVS: adrenal venous sampling. Hormonal data are at diagnosis of PA. a: PA diagnostic criteria is ≥63 nmol/24 h. b: PA diagnostic criteria is ≥500 pmol/L. For children at 2 months of age the upper normal limit of plasma aldosterone is 2500 pmol/L. c: PA diagnostic criteria is ≥64 pmol/mU.

of PA was made and treatment with spironolactone was started, with improvement of hypertension and hypokalemia. On CT scan, adrenals were normal and no nodules were identified. Spironolactone could be discontinued between 12 and 16 years of age without recurrence of major hypokalemia, but renin remained suppressed. Because of the reappearance of high blood pressure, spironolactone was reintroduced at age 19 years and 10 months. His blood pressure is currently well controlled. At 7 years of age the patient showed mild mental retardation, social skills alterations and learning disabilities. He was diagnosed 3 years later with multiplex developmental disorder. Brain MRI was normal and he didn't show any muscle weakness. Genetic screening for FH-I and FH-III was negative. His parents and siblings have no history of hypertension or hyperaldosteronism (Fig. 1A).

Patient K475-1 is a 64 years old male from the French West Indies. He was diagnosed with arterial hypertension at 36 years of age in a context of familial hypertension. His mother and three sisters were hypertensive. At age 51 years he was seen at the hypertension unit of the HEGP because of hypokalemia (2,7 mmol/L) associated with resistant hypertension. Biochemical analysis showed high levels of plasma and urinary aldosterone (965 pmol/L and 104 nmol/24 h, respectively) and low plasma renin (3,7 mU/L), confirming the diagnosis of PA. At CT scan, two nodules were identified on the right (21 mm) and left (11 mm) adrenals. AVS was performed showing a lateralization index of 48 on the left. The patient underwent left adrenalectomy with improvement of hypertension two months after surgery. The patient was lost at follow up and hormonal cure was not assessed. His younger sister (subject K475-2) showed resistant hypertension diagnosed at the age of 32 years, requiring 4 antihypertensive drugs to control blood pressure, associated with episodes of hypokalemia. At evaluation, she presented with high plasma aldosterone (804 pmol/L) and low plasma renin (2,6 mU/L). CT revealed no adrenal abnormality, but AVS was not performed and the patient was lost at follow up.

Patient K173-1 is a 64 years old male from West Indies. He was diagnosed with resistant hypertension at the age of 34 years, requiring three antihypertensive drugs to control blood pressure. His parents, two sisters, and one brother were also hypertensive (Fig. 1C). Diagnosis of PA was made at age 44 years in the presence of high plasma aldosterone (753 pmol/L) and low plasma renin (3 mU/L), without hypokalemia. There was no adrenal abnormality on CT scan. He did not continue the follow up in our department. His younger brother (K173-2) had a history of hypertension since age 39 years associated with hypokalemia (2,8 mmol/L) and obesity. Endocrine evaluation showed high plasma aldosterone (688 pg/mL) and suppressed plasma renin (<1 mU/L) levels. CT scan revealed left adrenal thickening without individualized adenoma. The patient was lost at follow up.

Patient K135-1 is a 60 years old female of European ancestry. She was diagnosed with hypertension at age 48 years with no history of familial hyperaldosteronism or hypertension. PA was diagnosed at age 50 years based on hypokalemia (2,5 mmol/L), high plasma aldosterone (620 pmol/L), high urinary aldosterone (118 nmol/24 h), and low plasma renin (1,5 mU/L). An 8 mm left adrenal nodule was identified on CT scan. AVS was not performed. The patient underwent left adrenalectomy with normalization of blood pressure and hormonal cure at 8 months of follow up (plasma aldosterone 269 pmol/L, plasma renin 12,9 mU/L, and blood pressure 121/76 mmHg without antihypertensive drugs). The resected adrenal showed an 8 mm large adenoma with predominance of zona fasciculata like cells. No somatic mutations were identified in *KCNJ5*, *CACNA1D*, *ATP1A1*, *ATP2B3*, or *CTNNB1*.

3.3. CACNA1H mRNA Expression in Normal Adrenal Cortex and APA

To investigate *CACNA1H* expression in the normal adrenal gland and APA, we retrieved mRNA expression data of L-type and T-type voltage-dependent calcium channels from a transcriptome study performed on 123 APA and 11 control adrenal cortices (Boulkroun et al., 2012). *CACNA1H* was highly expressed in both normal adrenal cortex and APA, being one of the most expressed T-type voltage-gated calcium channels (Table 3). No difference in *CACNA1H* mRNA expression was observed between normal adrenal cortex and APA.

3.4. Electrophysiological Analysis of Mutant Cav3.2 Channels

To assess the functional consequences of Cav3.2 variants on electrophysiological properties of the channels, we expressed wild type Cav3.2

Table 3
Expression of calcium channels in control adrenal cortex (CA) and aldosterone producing adenoma (APA)[a].

Gène	Protein	Type	CA	APA	*P* value
CACNA1C	Cav1.2	L-type	7.182	21.45	$P < 0.0001$
CACNA1D	Cav1.3	L-type	2.252	3.684	$P = 0.0607$
CACNA1I	Cav3.3	T-type	1.864	1.644	$P = 0.1148$
CACNA1H	Cav3.2	T-type	1.682	1.651	$P = 0.6029$
CACNA1E	Cav2.3	R-type	1.441	3.302	$P = 0.0009$
CACNA1A	Cav2.1	P/Q-type	1.272	3.399	$P < 0.0001$
CACNA1G	Cav3.1	T-type	0.6967	0.6747	$P = 0.6130$
CACNA1S	Cav1.1	L-type	0.5508	0.7413	$P = 0.9235$
CACNA1B	Cav2.2	N-type	0.5397	0.5753	$P = 0.5948$
CACNA1F	Cav1.4	L-type	0.4809	0.5642	$P = 0.3467$

[a] mRNA expression was retrieved from a transcriptome studies including 123 APA and 11 CA (Boulkroun et al., 2012). *P*-values indicate the differences between CA and APA.

($Cav3.2_{WT}$) and mutant channels ($Cav3.2_{196Leu}$, $Cav3.2_{1549Ile}$, $Cav3.2_{1951Glu}$ and $Cav3.2_{2083Leu}$) in tsA-201 cells and performed whole-cell patch clamp recordings. Fig. 2A shows typical T-type Ca^{2+} current recordings using depolarizing potentials (from −80 mV to +30 mV) from a holding potential (HP) at -100 mV, obtained on a cell expressing the $Cav3.2_{1549Ile}$ mutant (bottom traces), and compared to a family of control T-type currents ($Cav3.2_{WT}$, upper traces). The corresponding current-voltage (I—V) relationship obtained for the $Cav3.2_{1549Ile}$ mutant revealed a significant leftward shift in the voltage-dependent activation (Fig. 2B, blue trace) with a potential for half-activation ($V_{1/2}$) of −53.47 ± 0.77 mV, compared to the $V_{1/2}$ for activation of −43.81 ± 1.15 mV for the WT channels (see Table 4). No significant difference in the $V_{1/2}$ for activation was found for the three other mutants $Cav3.2_{196Leu}$, $Cav3.2_{1951Glu}$ and $Cav3.2_{2083Leu}$. Importantly, Ca^{2+} current kinetics of Cav3.2 channels were also markedly affected by the $Cav3.2_{1549Ile}$ mutation (Fig. 2A). Measurement of the time-constant for activation (Tau act, Fig. 2C) and inactivation (Tau inact, Fig. 2D) revealed significant slowing in activation and inactivation kinetics for $Cav3.2_{1549Ile}$ and $Cav3.2_{196Leu}$, while no change was observed for $Cav3.2_{1951Glu}$ and $Cav3.2_{2083Leu}$ (Table 4). Steady-state inactivation properties of Cav3.2 mutants were also affected (Fig. 3A), as evidenced by the significant leftward shift of the potential for half-inactivation ($V_{1/2}$, inact) for $Cav3.2_{1549Ile}$ (Table 4). In addition, a change in the inactivation slope constant (k) was identified for another mutant, $Cav3.2_{2083Leu}$, which exhibited significantly higher values for the inactivation slope factor, k (Table 4). Steady-state activation and inactivation properties of T-type calcium channels are crucial to determine the T-type "window current", a physiologically relevant Ca^{2+} entry that occurs in the range of the resting membrane potential (Rossier, 2016). Estimates of the window current for the four Cav3.2 mutants are presented in Fig. 3B, compared to the window current of WT Cav3.2 channels (black trace). A larger and more negatively shifted window current was observed for the $Cav3.2_{1549Ile}$ mutant, while the window current for the $Cav3.2_{2083Leu}$ mutant was reduced and shifted towards more positive membrane potential. In addition, while recovery from inactivation was significantly delayed for $Cav3.2_{1549Ile}$ (Fig. 3C, Table 4), it was significantly faster for the three other mutants, indicating that $Cav3.2_{196Leu}$, $Cav3.2_{1951Glu}$ and $Cav3.2_{2083Leu}$ mutations could favor larger Ca^{2+} entry during repetitive electrical activities (Table 4). In addition, deactivation kinetics was strongly slowed for $Cav3.2_{1549Ile}$ (Fig. 4D), compared to WT Cav3.2 channels and the three other Cav3.2 mutants. Analysis of the electrophysiological properties that could be affected by the Cav3.2 variants also identified a marked change in voltage-dependent facilitation (Fig. 4) for $Cav3.2_{196Leu}$, $Cav3.2_{1951Glu}$ and $Cav3.2_{2083Leu}$ (Fig. 4B), that is not observed for WT Cav3.2 channels (Fig. 4A). This paired-pulse protocol, using a depolarizing prepulse to +100 mV, revealed a marked increase in the current amplitude for these three mutants but not for $Cav3.2_{1549Ile}$ (Fig. 4C, Table 4), indicating that their activity could be enhanced during repetitive action potentials. Altogether, these electrophysiological data support a gain of channel activity for all four Cav3.2 mutants.

3.5. Effect of Cav3.2 Mutations on Aldosterone Biosynthesis

Aldosterone production was determined in adrenocortical H295R-S2 cells transiently transfected with $Cav3.2_{WT}$ or the mutant forms of Cav3.2 in basal condition and 24-hours after stimulation with angiotensin 2 (AngII) (10 nM) or K^+ (12 mM). In basal condition, a non-statistical significant increase of aldosterone production was observed in cells expressing the mutant forms of Cav3.2 compared to $Cav3.2_{WT}$ (Fig. 5A to D). Stimulation of cells with AngII or K^+ led to increased aldosterone production, compared to basal condition, in cells expressing WT or mutated channels (Fig. 5A to D). After K^+ stimulation cells overexpressing $Cav3.2_{1549Ile}$ and $Cav3.2_{196Leu}$ displayed a 4.5-fold ($Cav3.2_{1549Ile}$, $p < 0.0001$) and 2.5-fold ($Cav3.2_{196Leu}$, $p < 0.001$) higher increase of aldosterone biosynthesis compared to cells overexpressing $Cav3.2_{WT}$ (Fig. 5A and B); the levels of aldosterone were also increased by 40% in cells overexpressing the mutants $Cav3.2_{2083Leu}$ and $Cav3.2_{1951Glu}$,

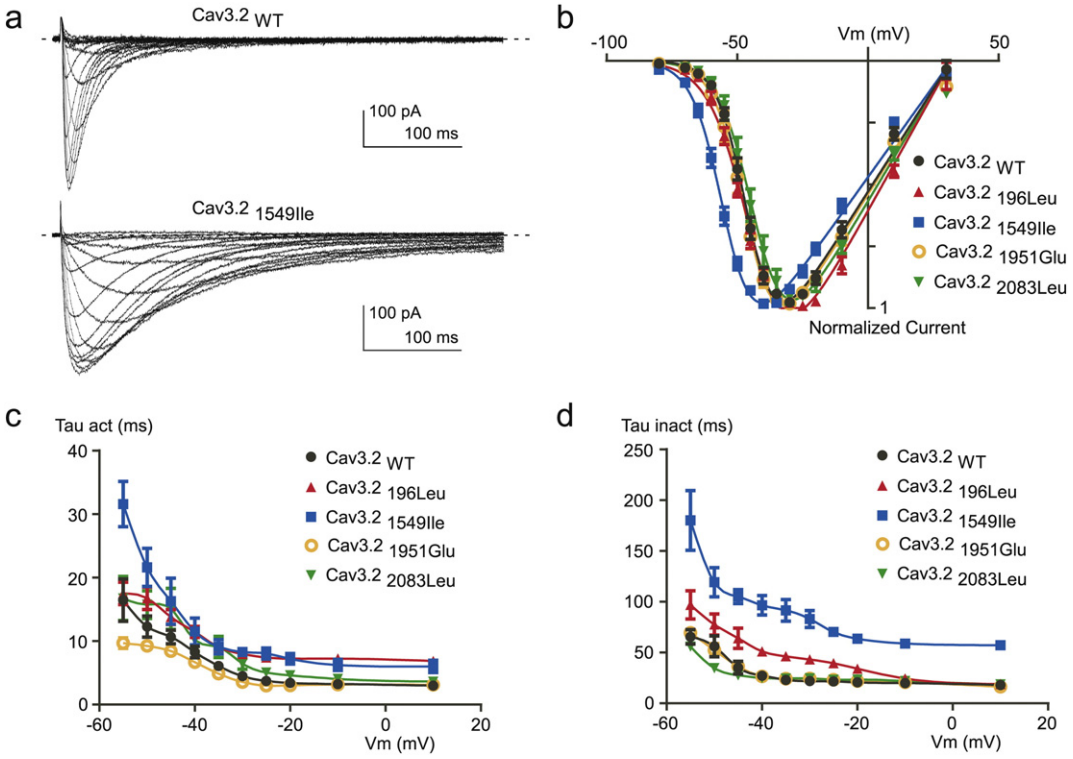

Fig. 2. Electrophysiological analyses of WT and mutant Cav3.2 channels. A. Representative families of Cav3.2 WT and $Cav3.2_{1549Ile}$ currents elicited by a series of depolarization steps ranging from −80 to +30 mV from a HP of −100 mV. The dotted line indicates the zero current level. B. Current-voltage (I–V) relationship obtained from experiments as illustrated in panel A for Cav3.2 WT and mutant Cav3.2 channels. C–D. Activation kinetics (C) and inactivation kinetics (D) as a function of the potential for Cav3.2 WT and mutant Cav3.2 channels.

Table 4
Electrophysiological properties of WT and mutant Cav3.2 channels.

	$Cav3.2_{WT}$	$Cav3.2_{196Leu}$	$Cav3.2_{1549Ile}$	$Cav3.2_{1951Glu}$	$Cav3.2_{2083Leu}$
Activation $V_{1/2}$ (mV)	−43.81 ± 1.15 (14)	−43.75 ± 1.06 (12)	−53.47 ± 0.77 (9)***	−45.95 ± 1.33 (8)	−42.42 ± 1.86 (9)
Activation slope (k, mV)	5.89 ± 0.48 (14)	6.62 ± 0.34 (12)	6.21 ± 0.31 (9)	5.69 ± 0.19 (8)	5.99 ± 0.34 (9)
Inactivation $V_{1/2}$ (mV)	−67.55 ± 1.42 (13)	−69.08 ± 1.47 (11)	−76.58 ± 0.93 (6)**	−67.98 ± 1.03 (6)	−73.11 ± 2.65 (6)
Inactivation slope (k, mV)	5.42 ± 0.36 (13)	5.87 ± 0.42 (11)	5.17 ± 0.22 (6)	4.19 ± 0.13 (6)	7.25 ± 0.64 (6)**
Activation kinetics @ −30 mV (Tau act, ms)	4.47 ± 0.33 (13)	7.99 ± 0.41 (14)**	8.30 ± 0.77 (9)**	3.57 ± 0.22 (8)	6.46 ± 0.86 (9)
Inactivation kinetics @ −30 mV (Tau inact, ms)	21.93 ± 2.09 (11)	43.23 ± 3.14 (12)***	83.07 ± 8.47 (7)***	24.52 ± 2.86 (8)	24.60 ± 2.23 (7)
Recovery (Tau, ms)	509.76 ± 30.00 (8)	419.12 ± 14.49 (9)*	1197.60 ± 93.92 (8)***	349.74 ± 15.63 (7)***	389.93 ± 28.89 (6)**
Deactivation kinetics @ −90 mV (Tau deact, ms)	3.01 ± 0.31 (15)	3.08 ± 0.28 (13)	11.67 ± 1.14 (9)***	2.50 ± 0.16 (12)	3.07 ± 0.35 (9)
Facilitation (fold increase normalized current)	1.12 ± 0.05 (8)	1.34 ± 0.03 (8)***	1.07 ± 0.02 (6)	1.26 ± 0.02 (9)**	1.35 ± 0.05 (9)***

Number of recorded cells are indicated in brackets.
* $P < 0.05$ compared with WT channels.
** $P < 0.01$ compared with WT channels.
*** $P < 0.001$ compared with WT channels.

without reaching statistical significance (Fig. 5C and D). No significant differences in aldosterone levels were observed in cells overexpressing the mutant forms of Cav3.2 compared to $Cav3.2_{WT}$ after stimulation with AngII (Fig. 5A to D).

3.6. Effect of Cav3.2 Mutations on mRNA Expression of Genes Coding for Key Proteins of Aldosterone Biosynthesis

In order to gain mechanistic insight into how mutant forms of Cav3.2 increased aldosterone production, we determined the effects of overexpressing WT and mutant channels on mRNA expression of genes coding for key proteins of aldosterone biosynthesis (*StAR* encoding Steroidogenic acute regulatory protein, *HSD3B1,* and *HSD3B2* encoding 3β-hydroxysteroid dehydrogenase isoform 1 and 2, *CYP21A2* encoding Steroid 21-hydroxylase, and *CYP11B2* coding for aldosterone synthase). In basal conditions, differences in mRNA expression were detected in cells transfected with $Cav3.2_{196Leu}$ but not with the other mutant channels (Fig. 6 and Fig. 7). Compared to cells transfected with $Cav3.2_{WT}$, cells overexpressing $Cav3.2_{196Leu}$ showed increased *StAR* (3-fold; $P < 0.01$), *HSD3B1* (3-fold; $P < 0.05$), and *CYP21A2* (2.3-fold ($P < 0.05$) mRNA expression (Fig. 6A, B and D); no differences were observed in *HSD3B2* or *CYP11B2* expression (Fig. 6C and E).

After K^+ stimulation, cells overexpressing $Cav3.2_{1549Ile}$ and $Cav3.2_{196Leu}$ showed increased mRNA expression of *StAR* ($Cav3.2_{1549Ile}$ 1.8 fold, $P < 0.05$; $Cav3.2_{196Leu}$ 2.8 fold, $P < 0.01$), *HSD3B1* ($Cav3.2_{1549Ile}$ 4.6 fold, $P < 0.05$; $Cav3.2_{196Leu}$ 6 fold, $P < 0.01$), *HSD3B2* ($Cav3.2_{1549Ile}$ 3 fold, $P < 0.05$; $Cav3.2_{196Leu}$ 4.1 fold, $P < 0.05$), *CYP21A2* ($Cav3.2_{1549Ile}$ 2.5 fold, $P < 0.05$; $Cav3.2_{196Leu}$ 2.4 fold, $P < 0.05$), and *CYP11B2* ($Cav3.2_{1549Ile}$ 4.7 fold, $P < 0.001$; $Cav3.2_{196Leu}$ 7.5 fold, $P < 0.001$) when compared to cells overexpressing $Cav3.2_{WT}$ (Fig. 6A–E). In cells expressing $Cav3.2_{1951Glu}$, K^+ stimulation induced an increase in *HSD3B1* (1.3 fold, $P < 0.05$), and *CYP11B2* (1.7 fold, $P < 0.05$) mRNA expression when compared with cells overexpressing $Cav3.2_{WT}$ (Fig. 7B and E), while K^+ stimulation of cells transfected with $Cav3.2_{2083Leu}$ lead to an

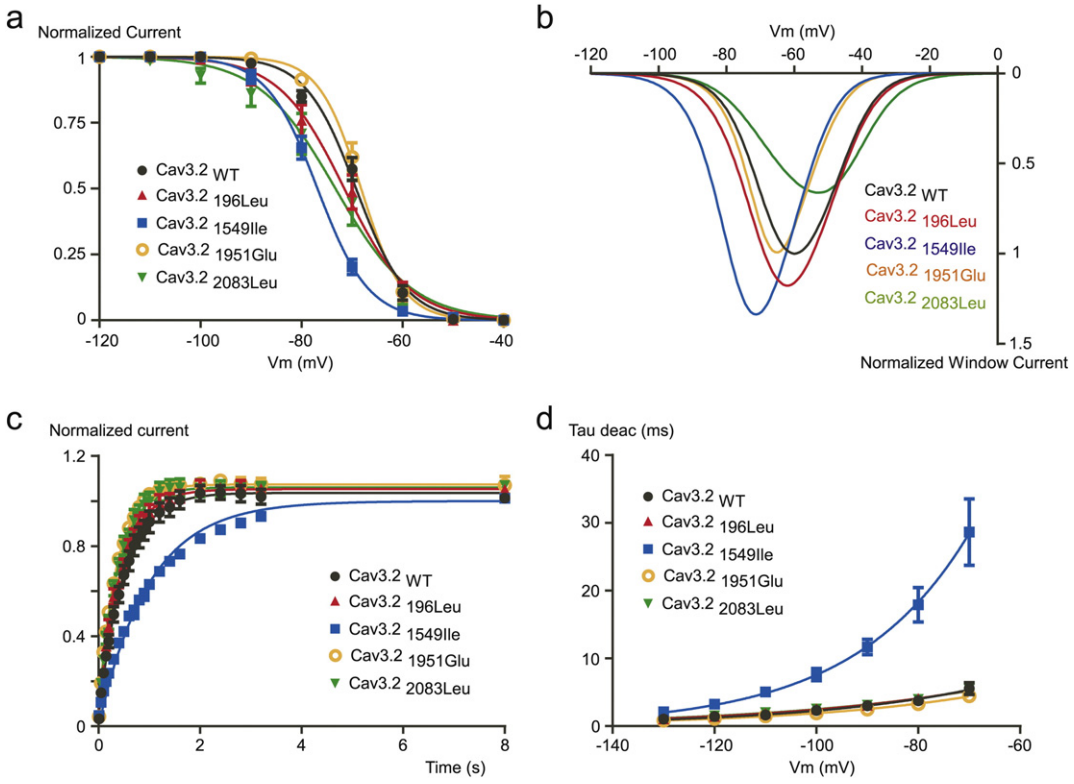

Fig. 3. Activation, inactivation and deactivation properties of WT and mutant Cav3.2 channels. A. Steady-state inactivation curves of Cav3.2 WT and mutant Cav3.2 channels. Currents were measured at −30 mV from HPs ranged from −120 to −40 mV (5 s duration, 10 mV increments). B. Simulated window currents of Cav3.2 WT and mutant channels. C. Recovery from inactivation of Cav3.2 WT and mutant Cav3.2 channels. Recovery from inactivation was measured at −30 mV after 1 s depolarization (−30 mV) applied from a HP of −100 mV of increasing duration (100 ms to 8 s). D. Deactivation kinetics as a function of the potential for Cav3.2 WT and mutant channels.

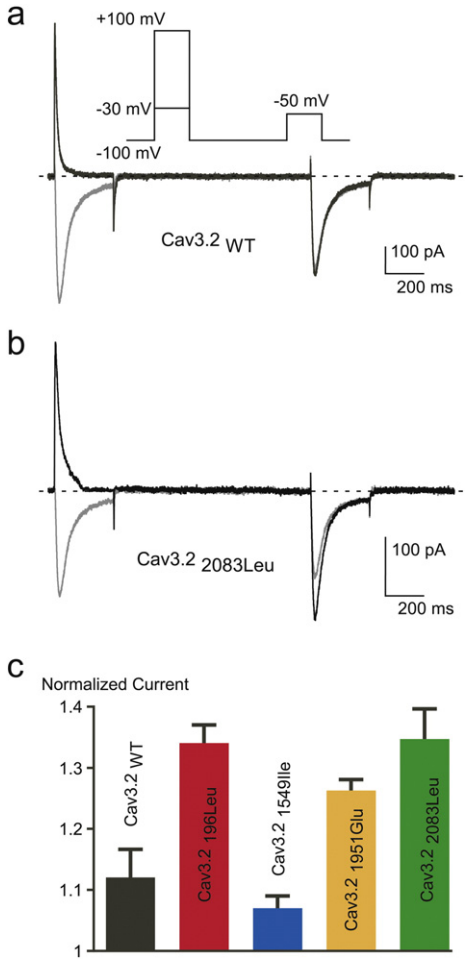

Fig. 4. Voltage dependent facilitation of Cav3.2 channels. A-B. Voltage-dependent facilitation of Cav3.2 WT (A) and Cav3.2$_{2083Leu}$ currents (B). To examine facilitation a 300 ms TP at −50 mV was preceded by a 300 ms conditioning pulse either at −30 mV or either at +100 mV. The interpulse interval was 1 s. The paired-pulse protocol was applied at a frequency of 0.066 Hz. C. Facilitation of Cav3.2 WT and mutant channels. The magnitude of facilitation is determined by the ratio of the current obtained after the +100 mV conditioning pulse to the current obtained after the −30 mV conditioning pulse.

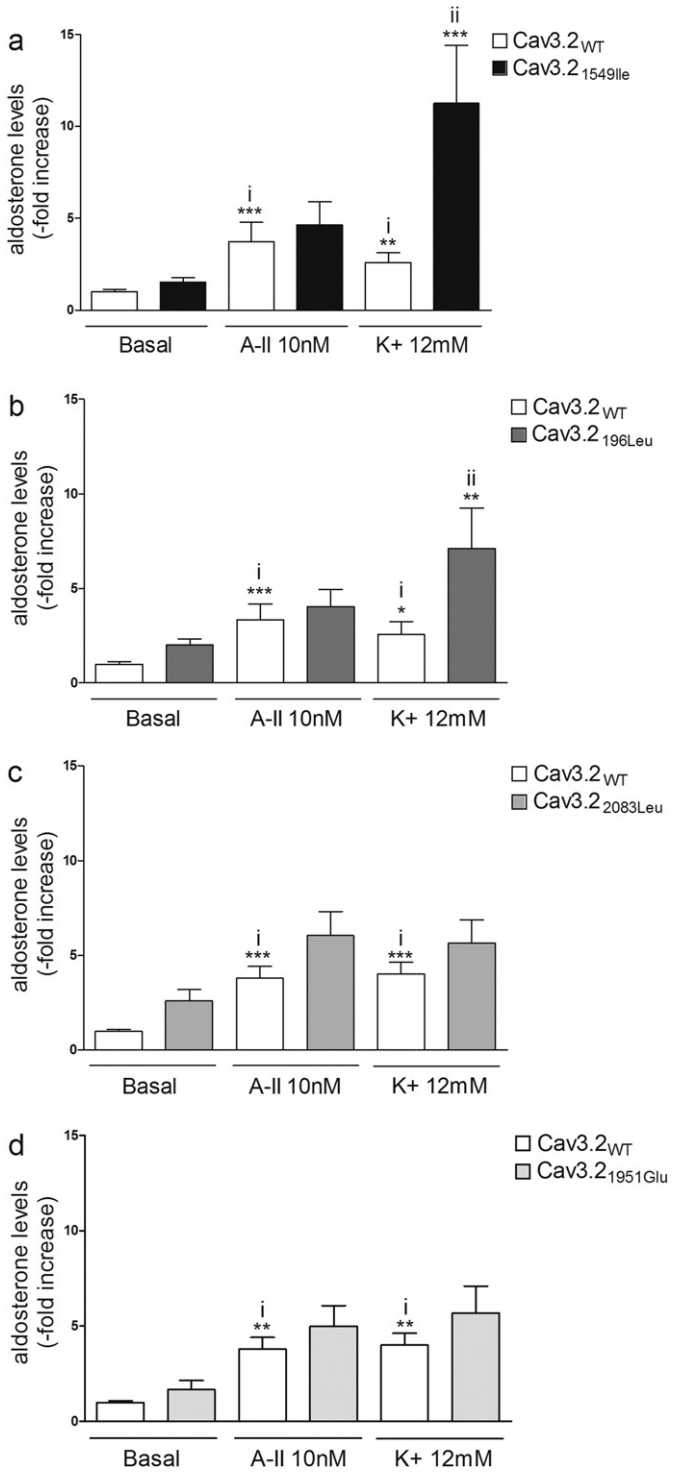

Fig. 5. Effect of WT and mutants Cav3.2 on aldosterone production. Basal and stimulated (AngII or K^+) aldosterone production by H295R-S2 cells transfected with WT or mutant Cav3.2$_{1549Ile}$ (A), Cav3.2$_{196Leu}$ (B), Cav3.2$_{2083Leu}$ (C), and Cav3.2$_{1951Glu}$ (D). 24 h post transfection, cells were serum deprived (0.1% Ultroser G) for 24 h and then incubated for another 24 h with fresh serum deprived medium in absence (basal) or presence of 10 nM of AngII (A-II 10 nM) or 12 mM K^+ (K^+ 12 mM). i) ***$P < 0.001$ or **$P < 0.01$ or *$P < 0.05$ vs Cav3.2$_{WT}$ basal; ii) ***$P < 0.001$ or **$P < 0.01$ vs Cav3.2$_{WT}$ K^+, $n = 9–12$.

increase in *StAR* (1.62 fold, $P < 0.01$), *HSD3B1* (2.1-fold, $P < 0.05$), and *CYP21A2* (2.3 fold, $P < 0.05$) (Fig. 7A, B, and D).

Treatment with AngII had no effect on *StAR*, *HSD3B1*, *HSD3B2*, *CYP21A2*, or *CYP11B2* expression in cells overexpressing Cav3.2$_{1549Ile}$ or Cav3.2$_{196Leu}$ compared with cells transfected with Cav3.2$_{WT}$ (Fig. 6A–E) and led to a slight decrease in *HSD3B1* (Cav3.2$_{2083Leu}$ − 32%, $P < 0.05$; Cav3.2$_{1951Glu}$ − 35%, $P < 0.05$) and *HSD3B2* (Cav3.2$_{2083Leu}$ − 30%, $P < 0.05$) mRNA expression in cells expressing the mutants Cav3.2$_{2083Leu}$ and Cav3.2$_{1951Glu}$ (Fig. 7B and C).

4. Discussion

Mutations in different genes coding for ion channels (*KCNJ5* (Choi et al., 2011) and *CACNA1D* (Azizan et al., 2013; Scholl et al., 2013)) and ATPases (*ATP1A1* and *ATP2B3* (Beuschlein et al., 2013)) have been identified in PA. They occur as somatic variants in the case of APA and germline variants in familial forms and affect regulation of intracellular ionic homeostasis and membrane potential, leading to activation of calcium signaling, the major trigger for aldosterone production (Azizan et al., 2013; Beuschlein et al., 2013; Choi et al., 2011; Fernandes-Rosa et al., 2014; Scholl et al., 2013). Despite these recent advances, the pathogenesis of a large proportion of APA and familial cases of PA has been elusive. The current study suggests that different genetic variants in *CACNA1H*, coding for the voltage-gated T-type calcium channel Cav3.2, may be responsible for PA with different phenotypic presentations. Through WES we have identified three *CACNA1H* germline variants in a patient with early onset PA and multiplex developmental disorder and in two patients diagnosed with FH-II. Additionally, we also

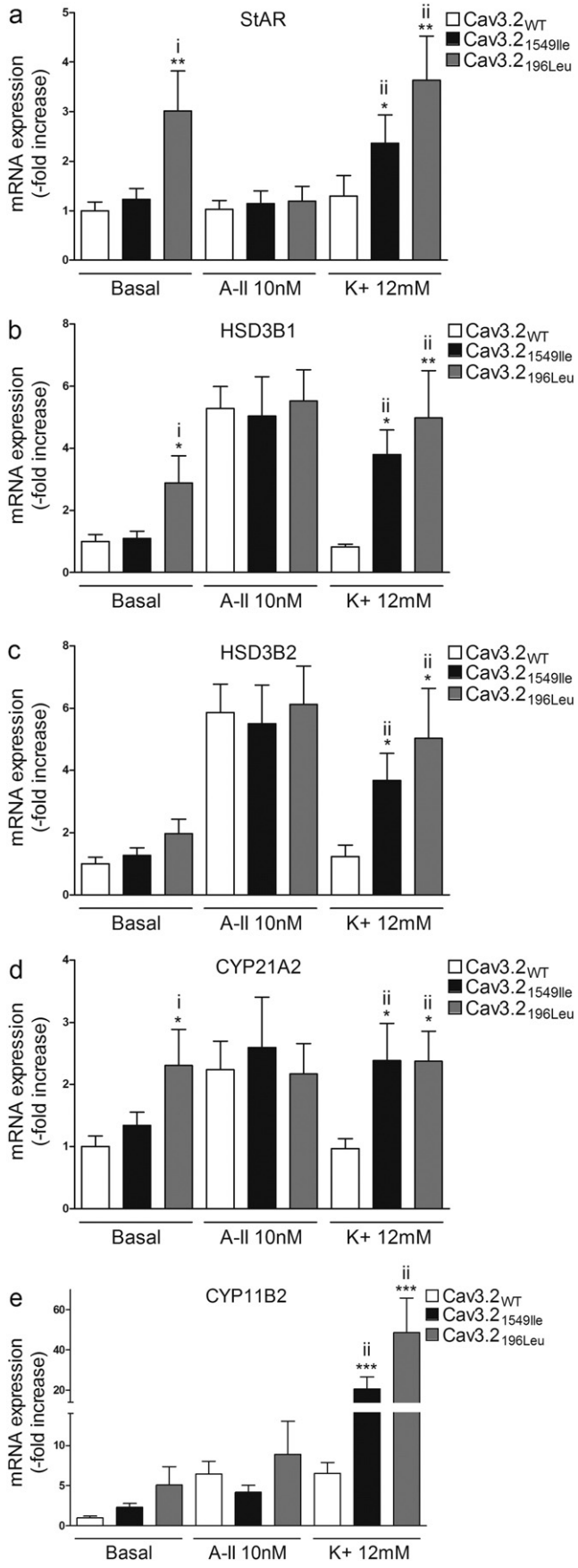

identified a germline *CACNA1H* variant in a patient with APA. These mutations lead to changes in electrophysiological channel properties, aldosterone production and/or expression of genes coding for steroidogenic enzymes, supporting a gain of function.

CACNA1H variants have been previously associated with epileptic disorders (such as childhood absence epilepsy, febrile seizures, myoclonic–astatic epilepsy, and juvenile absence epilepsy) (Chen et al., 2003; Heron et al., 2007; Khosravani et al., 2004; Khosravani et al., 2005), autism spectrum disorders (Splawski et al., 2006) and chronic pain in pediatric patients (Souza et al., 2016). More recently, a recurrent *CACNA1H* mutation, p.Met1549Val, has been identified in a cohort of patients with PA and hypertension before age 10 with no history of seizures, neurologic or neuromuscular disorders (Scholl et al., 2015). Family screening revealed autosomal dominant inheritance of the mutation with incomplete penetrance of the disease, including asymptomatic patients.

Our work enlarges the genetic and phenotypic spectrum of PA associated with *CACNA1H* mutations. In addition to early onset PA and hypertension, patient K055-3 carrying the p.Met1549Ile mutation presented mild mental retardation, social skills alterations and learning disabilities and was diagnosed with multiplex developmental disorder at age 10 years. This phenotype may owe to a gain of function effect of Cav3.2 in the nervous system, similar to what is observed in patients carrying germline mutations in another calcium channel gene, *CACNA1D*, coding for Cav1.3, who present with seizures and severe neurological abnormalities in addition to PA (Scholl et al., 2013). Among patients carrying the recurrent p.Met1549Val described previously (Scholl et al., 2015), developmental delay or attention deficit were reported in two mutation carriers. In our study, *CACNA1H* variants were also associated with familial hyperaldosteronism diagnosed as FH-II, and with sporadic PA and APA. This phenotypic variability may be explained by different functional consequences that the different *CACNA1H* variants have on channel properties. Differences in clinical presentation where also observed within family members carrying the recurrent *CACNA1H* p.Met1549Val variant, which were attributed to age-dependent variability or to genetic or environmental modifiers (Scholl et al., 2015). One limitation of the present study is the lack of follow-up data of patients with familial PA and more detailed clinical information on their relatives, which prevented deeper phenotype/genotype investigations in familial PA. Concerning the adrenal phenotype, the presence of additional somatic genetic variants occuring in the adrenal gland of patients carrying a germline *CACNA1H* variant may play a role in the development of APA, although no recurrent mutation in any of the known driver genes has been identified in tumor DNA of patient K135-1. Also, we cannot exclude that in some cases bilateral adrenal hyperplasia might occur in patients with PA, with a predominant aldosterone-producing nodule on one side leading to lateralization on AVS and cure after surgery. An alternative possibility is the involvement of adrenal aldosterone producing cell clusters (APCC), which have been shown to carry somatic mutations in APA driver genes in the normal population. Transition from APCC to APA, triggered by unknown factors and which has been evoked as a mechanism for APA development (Nishimoto et al., 2016) may be favored by germline genetic alterations, including *CACNA1H* variants, creating a favorable cellular environment for this transition.

Fig. 6. Effect of $Cav3.2_{196Leu}$ and $Cav3.2_{1549Ile}$ on mRNA expression of genes involved in aldosterone biosynthesis. 24 h post transfection, cells were serum deprived (0.1% Ultroser G) for 24 h and then incubated for another 24 h with fresh serum deprived medium in absence (basal) or presence of 10 nM of AngII (A-II 10 nM) or 12 mM K^+ (K^+ 12 mM). Cells were collected for RNA extraction, and real time RT-qPCR was performed. mRNA levels of *StAR, HSD3B1, HSD3B2, CYP21A2* and *CYP11B2* were normalized for *CACNA1H* expression to correct for transfection efficiency. Normalization for RNA quantity, and reverse transcriptase efficiency was performed against three reference genes (geometric mean of the expression of *18S* RNA, *HPRT*, and *GAPDH*). Data are represented as fold increase vs WT in basal condition. i) $^{**}P < 0.01$ or $^{*}P < 0.05$ vs $Cav3.2_{WT}$ basal; ii) $^{***}P < 0.001$ or $^{**}P < 0.01$ or $^{*}P < 0.05$ vs $Cav3.2_{WT}$ K^+, n = 9–12.

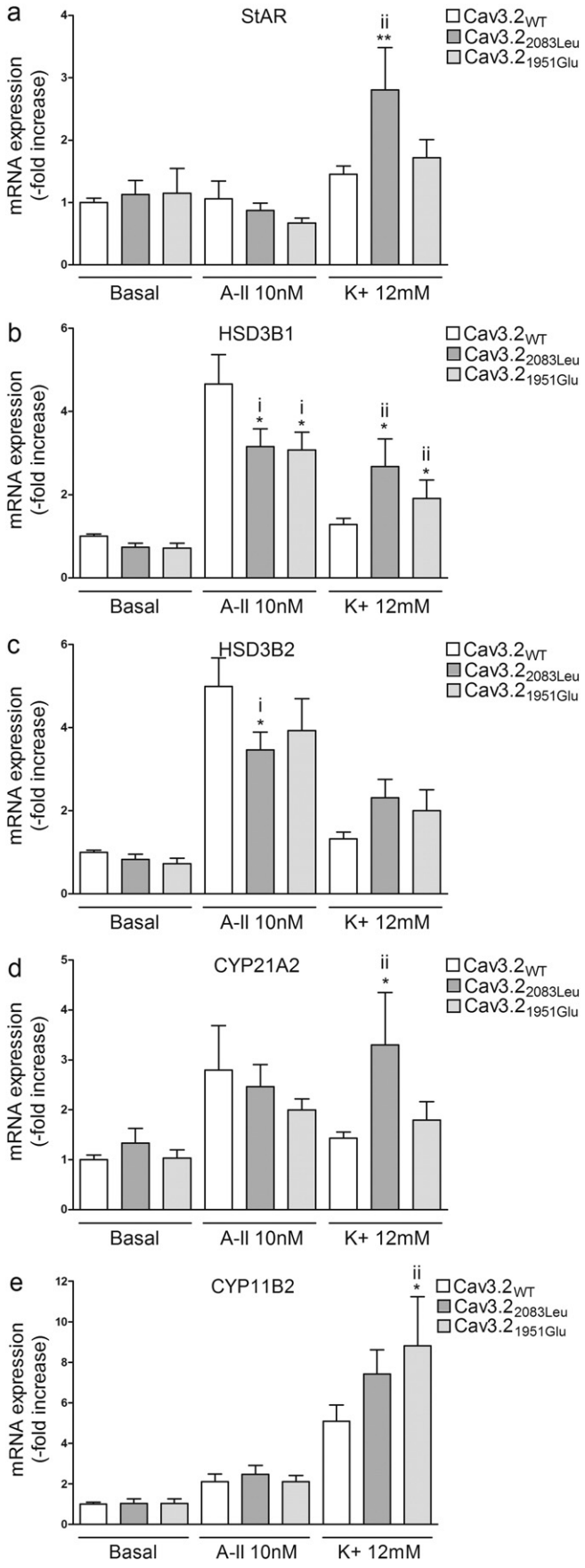

CACNA1H codes for the pore-forming channel protein Cav3.2, which consists of a single polypeptide chain of four homologous domains (I–IV), each one containing six transmembrane spans (Segments (S) 1–6), and cytoplasmic N- and C-termini. The pore of T-type channels is formed by the tetrameric arrangement of the four domains and it is lined by the S6 segment in the intracellular part, while the S4 segment serves as the voltage sensor (Perez-Reyes, 2003). The p.Ser196Leu mutation is located in the S4 segment of domain I. Each S4 segment contains positively charged residues on every third position and forms the voltage sensor, allowing the channel to open and close in response to changes in membrane potential (Burnay et al., 1994). The substitution of Leucine for Serine changes a polar uncharged aminoacid into a hydrophobic one, which is never found at this position (Burnay et al., 1994). A similar substitution from a polar uncharged to a hydrophobic residue has been found in the S4 segment of domain IV of a patient with idiopathic generalized epilepsy (p.Thr1733Ala) (Heron et al., 2007), while substitution from a positively charged to a hydrophobic amino acid in the S4 segment of domain I and II has been associated with autism spectrum disorders (Splawski et al., 2006). The mutation p.Met1549Ile is located in the S6 segment of domain III. A substitution of the same amino acid has recently been reported in five out of 40 subjects with hypertension and PA before age 10 years (Scholl et al., 2015). The p.Met1549Val mutation was shown to modify the functional properties of the calcium channel, facilitating its opening at more hyperpolarized potentials and delaying its inactivation, leading to increased aldosterone production (Reimer et al., 2016). Finally, variants p.Val1951Glu and p.Pro2083Leu are located at the cytoplasmic C-terminus of the channel. Studies on Cav3.1, which is closely related to Cav3.2, showed that the C-terminus determines fast inactivation of this T-type calcium channel (Staes et al., 2001). Amino acid substitutions in this region of Cav3.2 were found in patients with epilepsy (p.Arg1892His, p.Arg2005Cys, p.His2060Arg, p.Arg2077His) (Chen et al., 2003; Heron et al., 2007) and in autism spectrum disorders (p.Arg1871Gln + Ala1874Val) (Splawski et al., 2006).

Mutant Cav3.2 channels showed significant changes in their electrophysiological properties. $Cav3.2_{1549Ile}$, similarly to $Cav3.2_{1549Val}$ (Scholl et al., 2015), shows a significant shift in activation and inactivation properties towards more negative potentials. Consequently, $Cav3.2_{1549Ile}$ is activated at less depolarized membrane potentials close to the resting potential. In addition, this mutant channel exhibits a significant slowing of the activation, inactivation and deactivation kinetics which may greatly contribute to a larger increase in Ca^{2+} entry. These data suggest that, similar to Cav3.1, the Met-Phe-Val sequence of the S6 segment of domain III is implicated in rapid channel inactivation of Cav3.2 (Marksteiner et al., 2001). The three other mutants also show electrophysiological modifications, including slowing of activation and inactivation kinetics ($Cav3.2_{196Leu}$), altered steady-state inactivation ($Cav3.2_{196Leu}$ and $Cav3.2_{2083Leu}$) and increase in voltage-dependent facilitation ($Cav3.2_{196Leu}$, $Cav3.2_{1951Glu}$ and $Cav3.2_{2083Leu}$). The electrophysiological properties of these Cav3.2 mutants also suggest a gain of function phenotype. In idiopathic generalized epilepsy, gain of function mutations inside the voltage sensor S4 domain IV (p.Thr1733Ala) also showed a shift of the steady-state inactivation, in addition to a faster recovery from inactivation, while those in the cytoplasmic C-termini of the channel led to slightly faster activation in response to membrane

Fig. 7. Effect of $Cav3.2_{1951Glu}$ and $Cav3.2_{2083Leu}$ on mRNA expression of genes involved in aldosterone biosynthesis. 24 h post transfection, cells were serum deprived (0.1% Ultroser G) for 24 h and then incubated for another 24 h with fresh serum deprived medium in absence (basal) or presence of 10 nM of AngII (A-II 10 nM) or 12 mM K^+ (K^+ 12 mM). Cells were collected for RNA extraction and real time RT-qPCR was performed. mRNA levels of *StAR, HSD3B1, HSD3B2, CYP21A2* and *CYP11B2* were normalized for *CACNA1H* expression to correct for transfection efficiency. Normalization for RNA quantity, and reverse transcriptase efficiency was performed against three reference genes (geometric mean of the expression of *18S* RNA, *HPRT*, and *GAPDH*). Data are represented as fold increase vs WT in basal condition. i) $^*P < 0.05$ vs $Cav3.2_{WT}$ A-II; ii) $^{**}P < 0.01$ or $^*P < 0.05$ vs $Cav3.2_{WT}$ K^+, n = 9–12.

depolarization (p.Arg1892His) or decreased time-constant of recovery from inactivation (p.Arg2005Cys) (Heron et al., 2007).

Altogether, these results show that Cav3.2 mutations identified in patients with PA all induce changes in electrophysiological channel properties supporting a gain of channel activity, which is expected to generate increased electrical activity. Although qualitatively different, these modifications are inferred to increase calcium entry into the cell and to activate calcium signaling. Results from functional studies in adrenocortical H295R-S2 cells directly link electrophysiological abnormalities to increased aldosterone production. Indeed, transient transfections of $Cav3.2_{1549Ile}$ or $Cav3.2_{196Leu}$ led to significant increases in aldosterone production after stimulation with K^+, which was related to increased expression of genes coding for steroidogenic enzymes, including *CYP11B2*. Although $Cav3.2_{1951Glu}$ and $Cav3.2_{2083Leu}$ did not lead to significant increases in aldosterone biosynthesis, they also induced increased mRNA expression of a subset of genes coding for key proteins of aldosterone biosynthesis. We did not observe similar differences at the basal level (except for $Cav3.2_{196Leu}$) or after AngII stimulation. This might depend on the particular characteristics of H295R-S2 cells, which show high basal production of aldosterone that may mask subtle changes induced by Cav3.2 mutations at the basal state in a context of low transfection efficiency in these cells. Similarly, the fact that AngII mainly acts via inositol triphosphate-dependent calcium release from endoplasmatic reticulum (Burnay et al., 1994) very likely masks the effect of mutant channels on intracellular calcium levels. Stimulation of cells with K^+ appears to be more sensitive for the functional analysis of mutated voltage-dependent calcium channels, in particular for T-type calcium channels (Rossier et al., 1996). Indeed, K^+-stimulated aldosterone production from bovine zona glomerulosa cells is correlated with T-type channel activity (Schrier et al., 2001). The fact that Cav3.2 is the predominant T-type calcium channel in bovine and rat zona glomerulosa (Schrier et al., 2001), and in our transciptomic analysis in human adrenal cortex and APA, supports the role of Cav3.2 on increased aldosterone production in K^+-stimulated H295R-S2 cells.

In conclusion, we have identified four germline *CACNA1H* mutations in PA patients with different phenotypic presentations. These mutations induce significant changes in channel properties, aldosterone production and/or expression of genes coding for steroidogenic enzymes. Identification of new *CACNA1H* mutations that are associated with early onset PA and multiplex developmental disorder, familial forms diagnosed as FH-II or APA, suggests that *CACNA1H* might be a susceptibility gene predisposing to PA with different phenotypes, opening new perspectives for genetic diagnosis and management of patients with PA.

Funding Sources

This work was funded through institutional support from INSERM and by the Agence Nationale pour la Recherche (ANR Blanc 2011, No.: 11-BSV1 005 03, ANR-13-ISV1-0006-01), the Fondation pour la Recherche Médicale (DEQ20140329556), the Programme Hospitalier de Recherche Clinique (PHRC grant AOM 06179), and by grants from INSERM and Ministère Délégué à la Recherche et des Nouvelles Technologies.

Conflict of Interest

The authors have nothing to disclose.

Author Contributions

MCZ, FFR, GD, JC and PL designed experiments. TS, MCZ and FFR performed and analyzed whole exome sequencing. MCZ, GD, FFR and SB performed and analyzed in vitro studies on H295R-S2 cells. SB performed and analyzed gene expression studies. IB performed mutagenesis experiments. PL and JC performed and analyzed electrophysiology studies. MP, XJ, LA, and JB were responsible for patients' recruitment, medical care and clinical data acquisition. MCZ, GD, FFR, JC, PL, and MP wrote the manuscript. All authors revised the manuscript draft.

Appendix A. Supplementary Data

Supplementary data to this article can be found online at http://dx.doi.org/10.1016/j.ebiom.2016.10.002.

References

Adachi, M., Muroya, K., Asakura, Y., Sugiyama, K., Homma, K., Hasegawa, T., 2014. Discordant genotype-phenotype correlation in familial hyperaldosteronism type III with KCNJ5 gene mutation: a patient report and review of the literature. Horm. Res. Paediatr. 82 (2), 138–142.

Amar, L., Plouin, P.F., Steichen, O., 2010. Aldosterone-producing adenoma and other surgically correctable forms of primary aldosteronism. Orphanet. J. Rare Dis. 5, 9.

Azizan, E.A., Poulsen, H., Tuluc, P., et al., 2013. Somatic mutations in ATP1A1 and CACNA1D underlie a common subtype of adrenal hypertension. Nat. Genet. 45 (9), 1055–1060.

Beuschlein, F., Boulkroun, S., Osswald, A., et al., 2013. Somatic mutations in ATP1A1 and ATP2B3 lead to aldosterone-producing adenomas and secondary hypertension. Nat. Genet. 45 (4), 440–444 (444e441-442).

Boulkroun, S., Beuschlein, F., Rossi, G.P., et al., 2012. Prevalence, clinical, and molecular correlates of KCNJ5 mutations in primary aldosteronism. Hypertension 59 (3), 592–598.

Burnay, M.M., Python, C.P., Vallotton, M.B., Capponi, A.M., Rossier, M.F., 1994. Role of the capacitative calcium influx in the activation of steroidogenesis by angiotensin-II in adrenal glomerulosa cells. Endocrinology 135 (2), 751–758.

Bustin, S.A., Benes, V., Garson, J.A., et al., 2009. The MIQE guidelines: minimum information for publication of quantitative real-time PCR experiments. Clin. Chem. 55 (4), 611–622.

Calhoun, D.A., Nishizaka, M.K., Zaman, M.A., Thakkar, R.B., Weissmann, P., 2002. Hyperaldosteronism among black and white subjects with resistant hypertension. Hypertension 40 (6), 892–896.

Charmandari, E., Sertedaki, A., Kino, T., et al., 2012. A novel point mutation in the KCNJ5 Gene causing primary hyperaldosteronism and early-onset autosomal dominant hypertension. J. Clin. Endocrinol. Metab. 97 (8), E1532–E1539.

Chen, Y., Lu, J., Pan, H., et al., 2003. Association between genetic variation of CACNA1H and childhood absence epilepsy. Ann. Neurol. 54 (2), 239–243.

Choi, M., Scholl, U.I., Yue, P., et al., 2011. K^+ channel mutations in adrenal aldosterone-producing adenomas and hereditary hypertension. Science 331 (6018), 768–772.

Douma, S., Petidis, K., Doumas, M., et al., 2008. Prevalence of primary hyperaldosteronism in resistant hypertension: a retrospective observational study. Lancet 371 (9628), 1921–1926.

Dubel, S.J., Altier, C., Chaumont, S., Lory, P., Bourinet, E., Nargeot, J., 2004. Plasma membrane expression of T-type calcium channel alpha(1) subunits is modulated by high voltage-activated auxiliary subunits. J. Biol. Chem. 279 (28), 29263–29269.

Fernandes-Rosa, F.L., Williams, T.A., Riester, A., et al., 2014. Genetic spectrum and clinical correlates of somatic mutations in aldosterone-producing adenoma. Hypertension 64 (2), 354–361.

Funder, J.W., Carey, R.M., Fardella, C., et al., 2008. Case detection, diagnosis, and treatment of patients with primary aldosteronism: an endocrine society clinical practice guideline. J. Clin. Endocrinol. Metab. 93 (9), 3266–3281.

Funder, J.W., Carey, R.M., Mantero, F., et al., 2016. The management of primary aldosteronism: case detection, diagnosis, and treatment: an endocrine society clinical practice guideline. J. Clin. Endocrinol. Metab. 101 (5), 1889–1916.

Gomez-Sanchez, C.E., Foecking, M.F., Ferris, M.W., Chavarri, M.R., Uribe, L., Gomez-Sanchez, E.P., 1987. The production of monoclonal antibodies against aldosterone. Steroids 49 (6), 581–587.

Hannemann, A., Wallaschofski, H., 2012. Prevalence of primary aldosteronism in patient's cohorts and in population-based studies–a review of the current literature. Horm. Metab. Res. 44 (3), 157–162.

Heron, S.E., Khosravani, H., Varela, D., et al., 2007. Extended spectrum of idiopathic generalized epilepsies associated with CACNA1H functional variants. Ann. Neurol. 62 (6), 560–568.

Hubert, E.L., Teissier, R., Fernandes-Rosa, F.L., et al., 2011. Mineralocorticoid receptor mutations and a severe recessive pseudohypoaldosteronism type 1. J. Am. Soc. Nephrol. 22 (11), 1997–2003.

Khosravani, H., Altier, C., Simms, B., et al., 2004. Gating effects of mutations in the Cav3.2 T-type calcium channel associated with childhood absence epilepsy. J. Biol. Chem. 279 (11), 9681–9684.

Khosravani, H., Bladen, C., Parker, D.B., Snutch, T.P., McRory, J.E., Zamponi, G.W., 2005. Effects of Cav3.2 channel mutations linked to idiopathic generalized epilepsy. Ann. Neurol. 57 (5), 745–749.

Lafferty, A.R., Torpy, D.J., Stowasser, M., et al., 2000. A novel genetic locus for low renin hypertension: familial hyperaldosteronism type II maps to chromosome 7 (7p22). J. Med. Genet. 37 (11), 831–835.

Letavernier, E., Peyrard, S., Amar, L., Zinzindohoue, F., Fiquet, B., Plouin, P.F., 2008. Blood pressure outcome of adrenalectomy in patients with primary hyperaldosteronism with or without unilateral adenoma. J. Hypertens. 26 (9), 1816–1823.

Marksteiner, R., Schurr, P., Berjukow, S., Margreiter, E., Perez-Reyes, E., Hering, S., 2001. Inactivation determinants in segment IIIS6 of Ca(v)3.1. J. Physiol. 537 (Pt 1), 27–34.

Monticone, S., Hattangady, N.G., Penton, D., et al., 2013. A novel Y152C KCNJ5 mutation responsible for familial hyperaldosteronism type III. J. Clin. Endocrinol. Metab. 98 (11), E1861–E1865.
Mulatero, P., Bertello, C., Verhovez, A., et al., 2009. Differential diagnosis of primary aldosteronism subtypes. Curr. Hypertens. Rep. 11 (3), 217–223.
Mulatero, P., Tauber, P., Zennaro, M.C., et al., 2012. KCNJ5 mutations in European families with nonglucocorticoid remediable familial hyperaldosteronism. Hypertension 59 (2), 235–240.
Nishimoto, K., Seki, T., Kurihara, I., et al., 2016. Case report: nodule development from subcapsular aldosterone-producing cell clusters causes hyperaldosteronism. J. Clin. Endocrinol. Metab. 101 (1), 6–9.
Perez-Reyes, E., 2003. Molecular physiology of low-voltage-activated t-type calcium channels. Physiol. Rev. 83 (1), 117–161.
Reimer, E.N., Walenda, G., Seidel, E., Scholl, U.I., 2016. CACNA1HM1549V mutant calcium channel causes autonomous aldosterone production in HAC15 cells and is inhibited by Mibefradil. Endocrinology, en20161170.
Rossi, G.P., Bernini, G., Caliumi, C., et al., 2006. A prospective study of the prevalence of primary aldosteronism in 1,125 hypertensive patients. J. Am. Coll. Cardiol. 48 (11), 2293–2300.
Rossier, M.F., 2016. T-type calcium channel: a privileged gate for calcium entry and control of adrenal steroidogenesis. Front. Endocrinol. (Lausanne) 7, 43.
Rossier, M.F., Burnay, M.M., Vallotton, M.B., Capponi, A.M., 1996. Distinct functions of T- and L-type calcium channels during activation of bovine adrenal glomerulosa cells. Endocrinology 137 (11), 4817–4826.
Scholl, U.I., Nelson-Williams, C., Yue, P., et al., 2012. Hypertension with or without adrenal hyperplasia due to different inherited mutations in the potassium channel KCNJ5. Proc. Natl. Acad. Sci. U. S. A. 109 (7), 2533–2538.
Scholl, U.I., Goh, G., Stolting, G., et al., 2013. Somatic and germline CACNA1D calcium channel mutations in aldosterone-producing adenomas and primary aldosteronism. Nat. Genet. 45 (9), 1050–1054.
Scholl, U.I., Stolting, G., Nelson-Williams, C., et al., 2015. Recurrent gain of function mutation in calcium channel CACNA1H causes early-onset hypertension with primary aldosteronism. Elife 4, e06315.
Schrier, A.D., Wang, H., Talley, E.M., Perez-Reyes, E., Barrett, P.Q., 2001. alpha1H T-type Ca^{2+} channel is the predominant subtype expressed in bovine and rat zona glomerulosa. Am. J. Physiol. Cell Physiol. 280 (2), C265–C272.
So, A., Duffy, D.L., Gordon, R.D., et al., 2005. Familial hyperaldosteronism type II is linked to the chromosome 7p22 region but also shows predicted heterogeneity. J. Hypertens. 23 (8), 1477–1484.
Souza, I.A., Gandini, M.A., Wan, M.M., Zamponi, G.W., 2016. Two heterozygous Cav3.2 channel mutations in a pediatric chronic pain patient: recording condition-dependent biophysical effects. Pflugers Arch. 468 (4), 635–642.
Splawski, I., Yoo, D.S., Stotz, S.C., Cherry, A., Clapham, D.E., Keating, M.T., 2006. CACNA1H mutations in autism spectrum disorders. J. Biol. Chem. 281 (31), 22085–22091.
Staes, M., Talavera, K., Klugbauer, N., et al., 2001. The amino side of the C-terminus determines fast inactivation of the T-type calcium channel alpha1G. J. Physiol. 530 (Pt 1), 35–45.
Sukor, N., Mulatero, P., Gordon, R.D., et al., 2008. Further evidence for linkage of familial hyperaldosteronism type II at chromosome 7p22 in Italian as well as Australian and South American families. J. Hypertens. 26 (8), 1577–1582.
Sutherland, D.J., Ruse, J.L., Laidlaw, J.C., 1966. Hypertension, increased aldosterone secretion and low plasma renin activity relieved by dexamethasone. Can. Med. Assoc. J. 95 (22), 1109–1119.
Wang, T., Rowland, J.G., Parmar, J., Nesterova, M., Seki, T., Rainey, W.E., 2012. Comparison of aldosterone production among human adrenocortical cell lines. Horm. Metab. Res. 44 (3), 245–250.
Zennaro, M.C., Boulkroun, S., Fernandes-Rosa, F., 2015. Inherited forms of mineralocorticoid hypertension. Best Pract. Res. Clin. Endocrinol. Metab. 29 (4), 633–645.